


Observation of a π -Type Dipole-Bound State in Molecular Anions

Dao-Fu Yuan¹,* Yuan Liu¹,* Chen-Hui Qian¹, Yue-Rou Zhang¹, Brenda M. Rubenstein¹, and Lai-Sheng Wang¹†
 Department of Chemistry, Brown University, Providence, Rhode Island 02912, USA

 (Received 9 April 2020; revised 7 June 2020; accepted 28 July 2020; published 14 August 2020)

We report the observation of a π -type dipole-bound state (π -DBS) in cryogenically cooled deprotonated 9-anthrol molecular anions ($9AT^-$) by resonant two-photon photoelectron imaging. A DBS is observed 191 cm^{-1} (0.0237 eV) below the detachment threshold, and the existence of the π -DBS is revealed by a distinct ($s + d$)-wave photoelectron angular distribution. The π -DBS is stabilized by the large anisotropic in-plane polarizability of $9AT$. The population of the dipole-forbidden π -DBS is proposed to be via a nonadiabatic coupling with the dipole-allowed σ -type DBS mediated by molecular rotations.

DOI: [10.1103/PhysRevLett.125.073003](https://doi.org/10.1103/PhysRevLett.125.073003)

Neutral molecules can capture an excess electron to form stable molecular anions [1]. The mechanisms and strength of the electron binding can differ drastically. Conventional anions are valence bound and the electron binding is dominated by short-range interactions. However, long-range interactions can also facilitate weak electron binding [2–4], forming noncovalent anions. If the neutral molecular core possesses a large dipole moment beyond a critical value ($\sim 2.5\text{ D}$) [4–8], an extra electron can be bound by the dipolar potential ($\sim 1/r^2$), forming so-called dipole-bound states (DBSs) [2–12]. If the neutral core has a vanishing dipole moment, but a large quadrupole moment, a quadrupole-bound state (QBS) can be formed [13–15]. Electronic bound states have also been predicted and observed for molecules with electrostatic multipoles [16], whereas electron correlation effects can lead to correlation-bound states (CBSs) [17–22]. If polarization effects are dominating, the resulting anions are dubbed polarization-bound states (PBSs) [23] or image-charge-bound states in cases of metal clusters [24,25]. Because of the long-range nature of these interactions, the electron binding energies in these noncovalent anions are usually quite small with very diffuse electronic wave functions.

Besides the weakly bound nature of these noncovalent states, relatively little is known about the characteristics of their wave functions. Wallis *et al.* predicted for a fixed dipole field the existence of a series of DBSs characterized by three quantum numbers, $(n_\lambda n_\mu m)$, representing the number of nodes in the radial, polar, and azimuthal directions, respectively; a π -type DBS (π -DBS) exists as an excited electronic state in addition to the σ -type ground state [26]. Critical dipole moments for different quantum states of the DBSs were also calculated for a fixed dipole field [4,27]. Recently, Jordan and co-workers predicted the existence of π -type weakly bound excited states in $(\text{NaCl})_2^-$ [28] and large fullerenes [29]. Experimentally, all previous photoelectron imaging studies of noncovalent states have revealed p -wave angular

distributions [21,22,30–36], suggesting these states consist of σ -type orbitals with no angular nodes. Using scanning tunneling microscopy, Feng *et al.* observed superatom molecular states in C_{60} absorbed on copper surfaces with s , p , and d angular nodes [37], which are essentially PBSs or image-charge bound states [24,25]. However, π -type noncovalent states have never been observed in isolated molecular systems. Noncovalent states have been proposed as the “doorway” to the formation of valence-bound anions [38,39], especially for those formed during the DNA damage process by low-energy electron attachment [40] and in the interstellar medium under astronomical environments [41]. The observation of a π -type DBS would not only confirm the theoretical predictions of its existence, but would also be important for understanding the electron capture mechanisms via DBS to form anions. Moreover, noncovalent states with angular nodes in their wave functions make it possible for them to be used as new molecular qubits for quantum information science applications beyond Rydberg atoms [42]. Polycyclic aromatic compounds are promising candidates to search for the π -type DBS, because their dipole moments can be tuned readily by heteroatom substitutions [8] and their high polarizabilities provide additional molecular interactions [19,20].

Here we report the observation of a π -DBS in deprotonated 9-anthrol ($9AT^-$, $\text{C}_{14}\text{H}_9\text{O}^-$, see inset in Fig. 1). $9AT^-$ is a stable valence-bound anion and the π -DBS is observed as an excited state of the anion just below the detachment threshold, because the $9AT$ core has a dipole moment of 3.6 D. The π -DBS is stabilized preferentially relative to the σ -DBS by the polarization effects. A nonadiabatic process transferring population from the dipole-allowed σ -DBS to the dipole-forbidden π -DBS mediated by molecular rotations is proposed to explain the ($s + d$)-wave angular distributions observed in the resonant two-photon detachment (R2PD) spectrum.

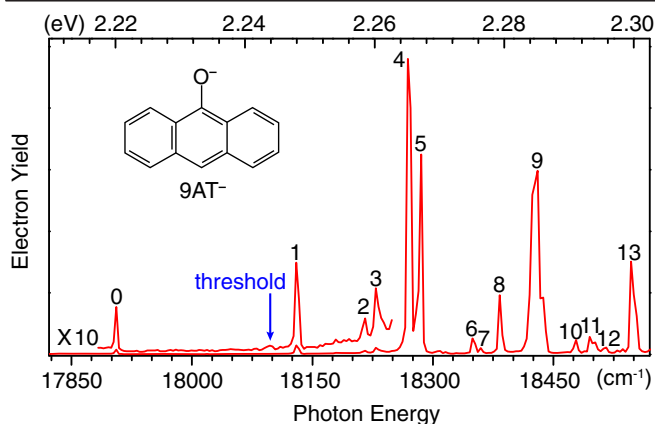


FIG. 1. The photodetachment spectrum of $9AT^-$ by measuring the total electron yield as a function of photon energy. The arrow indicates the detachment threshold at $18\,097\text{ cm}^{-1}$ (2.2437 eV).

The experiment was carried out using an electrospray photoelectron spectroscopy (PES) apparatus [43] equipped with a cryogenically cooled Paul trap [44] and a high-resolution photoelectron (PE) imaging system [45]. More experimental details are given in the Supplemental Material [46]. Nonresonant PE spectra of $9AT^-$ were obtained at two photon energies (Figs. S1 and S2 in the Supplemental Material [46]) and yielded an accurate electron affinity (EA) of $18\,097 \pm 3\text{ cm}^{-1}$ ($2.2437 \pm 0.0004\text{ eV}$) for neutral $9AT$. To search for the anticipated DBS, we scanned the wavelength of the detachment laser and monitored the electron yield as a function of photon energy near the detachment threshold (Fig. 1). The blue arrow at $18\,097\text{ cm}^{-1}$ represents the detachment threshold, measured from the nonresonant PE spectrum [46]. Indeed, we observed a weak peak below the threshold, labeled as 0 at $17\,906\text{ cm}^{-1}$ (2.2201 eV) in Fig. 1. This below-threshold peak is observed via R2PD, similar to those observed previously [30–34,47–49]. Since there is no more transition below peak 0, it should represent the ground vibrational level of the expected DBS. The binding energy of the DBS is determined to be $191 \pm 3\text{ cm}^{-1}$ ($0.0237 \pm 0.0004\text{ eV}$) relative to the detachment threshold. The baseline above threshold in Fig. 1 represents contributions from single-photon nonresonant detachment processes. Furthermore, thirteen prominent above-threshold peaks are observed (1–13 in Fig. 1), due to autodetachment from higher vibrational levels of the DBS to specific vibrational levels of the neutral radical, as shown previously [30–34,47–49]. The excitation wavelengths and energy shifts of all the above-threshold peaks relative to the ground vibrational level of the DBS are summarized in Table S1 [46].

By tuning the detachment laser to the above-threshold resonances in Fig. 1, we obtained resonantly enhanced PE spectra, three of which are presented in Fig. 2. The remaining data are shown in Fig. S3 of the Supplemental Material [46]. Generally, two detachment channels

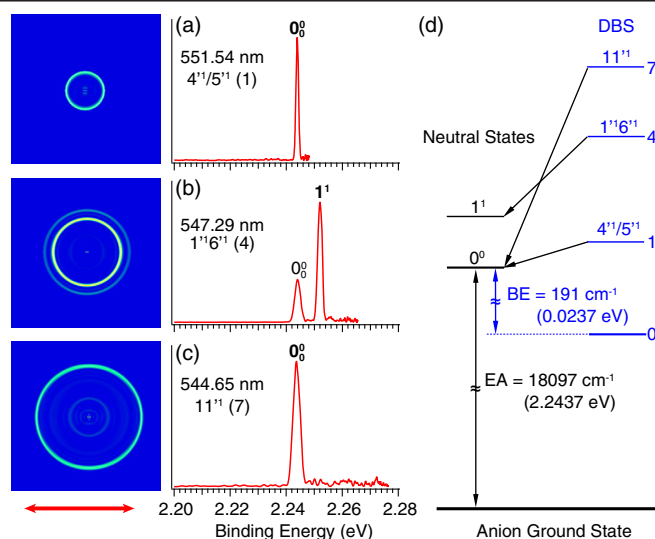


FIG. 2. Resonant PE images and spectra of $9AT^-$ at (a) 551.54 nm ($18\,130\text{ cm}^{-1}$ or 2.2478 eV), (b) 547.29 nm ($18\,272\text{ cm}^{-1}$ or 2.2654 eV), and (c) 544.65 nm ($18\,362\text{ cm}^{-1}$ or 2.2766 eV). The DBS vibrational levels and the corresponding peak number in Fig. 1 are given. The autodetachment-enhanced peaks are labeled in boldface. (d) Schematic energy level diagram for autodetachment from three DBS vibrational levels of $9AT^-$ to the related neutral final states, corresponding to the spectra in (a)–(c). The double arrow below the images indicates the direction of the laser polarization.

contribute to the resonant PE spectra: the nonresonant photodetachment represented by the weak baseline above the detachment threshold and resonantly enhanced autodetachment via vibrational levels of the DBS. Figure 2(a) shows the resonant PE spectrum at peak 1 of Fig. 1, representing excitation from the ground state of $9AT^-$ to the 4^1 or 5^1 vibrational level of the DBS (the prime denotes the vibrational modes of the DBS). Since modes ν_4 and ν_5 of $9AT$ have nearly the same computed vibrational frequencies (Table S2 [46]), we could not assign peak 1 definitively. Transfer of the vibrational energy to the DBS electron via vibronic coupling induces the autodetachment, resulting in an enhanced 0_0^0 peak in Fig. 2(a). Similar processes happen in Fig. 2(c), corresponding to autodetachment from excitation of 11^1 in the DBS. It is also possible to excite combinational vibrational levels of the DBS. Figure 2(b) shows excitation to the $1^1 6^1$ combinational level. Coupling of one quantum of the ν_6^1 mode (6^1) results in the enhanced 1^1 peak in the PE spectrum in Fig. 2(b). The vibronic coupling follows the $\Delta v = -1$ propensity rule [50,51] because the DBS electron has very little influence on the structure of neutral $9AT$. The autodetachment processes are summarized in Fig. 2(d), where autodetachment to related neutral vibrational levels are indicated by arrows. The resonant PE spectra and the corresponding enhanced vibrational peaks in Fig. S3 are readily understood similarly using the computed

vibrational frequencies in Table S2 [46]. In several spectra, more than one assignment is possible due to the overlap of several vibrational levels. The $\Delta v = -1$ propensity rule was based on the harmonic approximation [50,51] and can be violated due to anharmonicity [49,52]. A complete assignment of the observed vibrational resonances is summarized in Table S1 and the corresponding autodetachment processes are shown in Fig. S4 of the Supplemental Material [46].

Tuning the detachment laser to peak 0 in Fig. 1, we obtained the R2PD image of 9AT^- , as shown in Fig. 3(a). A single sharp peak at low binding energy was expected, but the observed spectrum was more complicated. For comparison, we show in Fig. 3(b) the R2PD spectrum of phenoxide (PhO^-), which was known to have a DBS 97 cm^{-1} below the detachment threshold [30,34]. The low binding energy peak (σ -DBS) represents detachment from the DBS of PhO^- and should have a binding energy of 97 cm^{-1} (0.0120 eV). The R2PD images in both cases show a bright spot in the center, representing photoelectrons with very low kinetic energies, labeled as E_{hb} in the PE spectra. This observation suggests a process where the electronic energy in the DBS is converted to the vibrational manifold of the anion ground electronic state upon the absorption of the first photon, followed by fast intramolecular vibrational energy redistribution [53]. The low energy electrons come from detachment from these

vibrationally excited levels of the ground electronic state of the anion by a second photon within the same laser pulse. Such electronic to vibrational energy conversion from the DBS to the ground electronic state of the anion has been observed in several complex anions that we have examined previously [33,34,47–49]. The existence of the long tails extending to lower binding energies of these features is consistent with the vibrational relaxation, which should occur on a timescale of picoseconds, much shorter than our laser pulse width ($\sim 6\text{ ns}$). However, the lifetimes of the lower vibrational levels may be sufficiently long such that they appear as the “vibrational hot bands” to the second photon in the sequential two photon process.

The lowest binding energy peak in Fig. 3(a) should come from the R2PD process, and its binding energy should represent that of the DBS of 9AT^- , i.e., 191 cm^{-1} (0.0237 eV) [Fig. 2(d)]. However, there are additional features beyond the DBS peak. In particular, there is a well-resolved and relatively intense peak (VE) at 0.225 eV (1815 cm^{-1}), followed by more weak peaks akin to a vibrational progression. These features are assigned to photodetachment from a valence excited (VE) state of 9AT^- by a second photon. This excited state is populated due to relaxation from the DBS upon absorption of the first photon via intersystem crossing from the DBS to a triplet valence excited state of 9AT^- . Such intersystem crossing from DBS to VE states has been observed recently in the deprotonated biphenol anion [54]. Indeed, our theoretical calculations located a triplet VE state 1.5 eV above the anion ground state (Table S3 [46]), in qualitative agreement with our observation. We also did a Franck-Condon simulation from the triple VE state to the final neutral state (Fig. S5). The good agreement between the simulation and the experimental data provides further support for our assignment of the additional spectral features in the R2PD spectrum [Fig. 3(a)].

The most surprising difference between the R2PD data of 9AT^- and PhO^- is their angular distributions. The R2PD image of PhO^- exhibits a p -wave angular distribution (i.e., parallel to the laser polarization) with a positive anisotropy parameter close to 2 ($\beta = 1.3$) [30], as expected from the σ orbital of the DBS. Similar p -wave angular distributions have been observed for all R2PD images via DBS that have been reported previously [21,22,30–36,47–49]. However, the R2PD image for 9AT^- displays a distinct *perpendicular* distribution, which represents a ($s + d$)-wave angular distribution with a negative β value ($\beta = -0.7$). This unexpected observation suggests that the second photon in the R2PD detaches an electron from a π -DBS [55].

Molecules with sufficiently large dipoles may possess more than one bound DBS. Early studies of a fixed dipole concluded that 4.5 D is required for the second DBS (σ -type), and 9.64 D is required for the first π -type DBS [4,26,27,56,57]. However, higher DBSs have not been

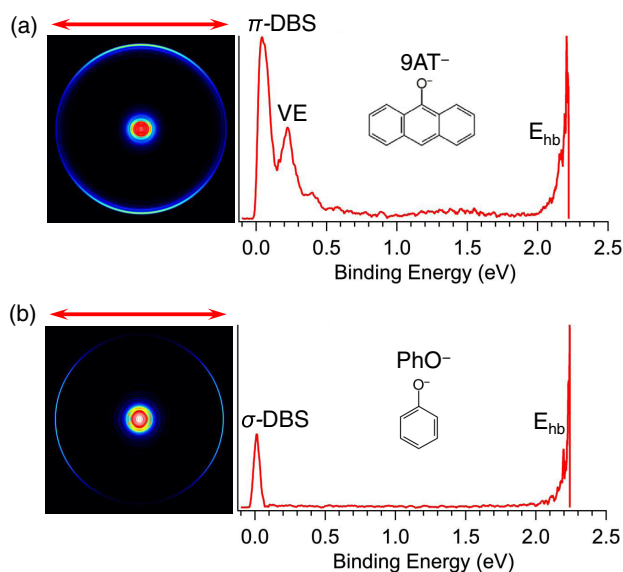


FIG. 3. Photoelectron images and spectra of (a) 9AT^- and (b) PhO^- from R2PD via the vibrational ground states of their respective DBS. The double arrows above the images represent the laser polarization. Note the photoelectron angular distribution of the R2PD is perpendicular to the laser polarization for 9AT^- , but parallel to the laser polarization for PhO^- . Peaks labeled as VE and E_{hb} represent photoelectrons detached from a valence excited state (in the case of 9AT^-) and excited vibrational levels of the ground electronic states of the anions, respectively.

observed experimentally, even for systems with dipole moment as large as 6.2 D [58]. Thus, a bound higher-lying π -type DBS for 9 AT ($\mu = 3.6$ D) was not expected, though it might exist as an above-threshold resonance, similar to the correlation-bound states in $(\text{NaCl})_2^-$ [28]. To understand the nature of the DBS in 9AT^- , we carried out further theoretical calculations [46]. Our calculations indeed suggest the possible existence of both bound σ - and π -type DBSs in 9AT^- and PhO^- , with the π -DBS higher in energy than the σ -DBS by a few meV in 9AT^- and PhO^- (Table S5 [46]). Figure 4 displays the wave functions of the σ - and π -DBS in 9AT^- [panel (a)] and the σ -DBS in PhO^- [panel (b)]. In the σ -DBS, the diffuse electron density is found mostly away from the molecular core and on the positive side of the dipole with no angular node in the azimuthal direction (along the z axis). The π -DBS of 9AT^- , on the other hand, possesses one angular node and is found mostly on both sides of 9AT (along the y axis), perpendicular to the dipole axis. The wave function of the π -DBS of PhO^- (not shown) is similar.

It is important to point out that under the C_{2v} point group symmetry the transitions from the anion ground states (A_1 symmetry) to the σ -DBSs (B_1 symmetry) in both 9AT^- and PhO^- are dipole allowed, while those to the π -DBSs (A_2 symmetry) are dipole forbidden [59]. However, the angular distribution of the R2PD in Fig. 3(a) for 9AT^- indicates detachment from the π -DBS by the second photon. Because of the dipole-forbidden nature of the π -DBS in 9AT^- , the first photon

in the R2PD must populate the σ -DBS. A question immediately arises: how is the population in the σ -DBS transferred to the π -DBS?

The differences between the molecular structures of 9AT and PhO and their electrostatic moments and polarizabilities provide hints to this question. Multipole expansion of the charge distributions of 9AT and PhO shows that 9AT has a smaller dipole, but larger quadrupole and octupole moments, compared to PhO (Table S6 [46]). However, the biggest difference between the two species lies at their polarizabilities (Table S7 [46]): the average polarizability of 9AT is more than twice as large as that of PhO. The large polarizability of 9AT must contribute significantly to the electron binding in the DBS, because the binding energy of the DBS in 9AT^- (191 cm^{-1}) is much larger than that in PhO^- (97 cm^{-1}), even though the dipole moment of 9AT (3.6 D) is smaller than that of PhO (4.0 D) [30]. In particular, the in-plane component of the polarizability α_{yy} in 9AT is huge, due to the delocalized π electrons across the anthracene ring. This large α_{yy} value is expected to preferentially stabilize the in-plane π -DBS [Figs. 4(a)], which is along the y axis, thus making it energetically close to or even lower than the σ -DBS. Note that this stabilization due to the polarization effect is not fully captured by our time-dependent DFT calculation, which overestimated the DBS binding energies, in particular for PhO^- (Table S5 [46]).

The near degeneracy of the σ - and π -DBS in 9AT^- provides a plausible mechanism for the population transfer from the σ -DBS to the π -DBS. This process can be viewed as a split of the σ -DBS wave function into two halves and each part is stabilized by the large polarizability along the y axis (α_{yy}). This wave function splitting must be mediated by a perturbation which should carry angular momentum to allow the nodal structure of the DBS wave function to change from the σ - to π -type (i.e., the conservation of angular momentum). This perturbation is likely provided by molecular rotations. The rotational temperature of anions in our ion-trap is known to be 30–35 K [47], which means that most 9AT^- anions are in rotationally excited states. Since the β value (-0.7) of the angular distribution in the R2PD [π -DBS in Fig. 3(a)] is close to the atomic limit of -1 , we infer that the photoelectron signals detached from the σ -DBS should have minimal contribution, suggesting that the initially-populated σ -DBS is mostly converted to the π -DBS before the absorption of the second photon within our laser pulse width (~ 6 ns). A schematic illustration of the different R2PD processes in 9AT^- and PhO^- are shown in Fig. 4(c), where the nonadiabatic population transfer (NAPT) is indicated by a dashed arrow. As mentioned above, our DFT calculations cannot accurately predict the energetic positions of the π -DBS. But it is safe to say that the π -DBS in PhO^- must be higher in energy than the σ -DBS and similar NAPT cannot occur in this less polarizable system. Since the coupling with

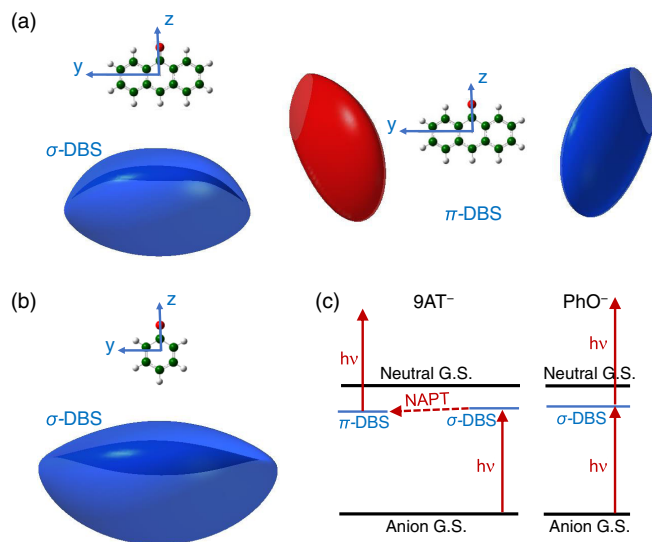


FIG. 4. The DBS wave functions of (a) 9AT^- and (b) PhO^- , as well as (c) a schematic diagram of the R2PD processes via the DBS of the two anions from the anion ground state (G.S.). Note the proposed nonadiabatic population transfer (NAPT) from the σ - to π -DBS in 9AT^- in (c). The DBS wave functions are plotted at an isovalue of 0.0034. The coordinate system is chosen such that the dipole moment is along the z axis.

molecular rotations is the key to mediate the conversion from the σ - to π -DBS, the timescale for the NAPT should be on the order of ps, much shorter than our detachment laser pulse width.

In conclusion, we report the observation of a π -type dipole-bound excited state in 9AT^- , stabilized by the anisotropic polarizability of 9AT . Resonant two-photon photoelectron imaging via the DBS of 9AT^- reveals an unexpected ($s + d$)-wave angular distribution, suggesting detachment from a π -type DBS. Theoretical calculations indicate that the unique molecular structure and large in-plane polarizability of the 9AT molecule help stabilize the π -DBS. The initially populated dipole-allowed σ -DBS is converted to the dipole-forbidden π -DBS via nonadiabatic coupling with the rotational degrees of freedom. The observation of different weakly bound states in the same molecule and their sensitivity to molecular structures make it possible to control molecular quantum states via molecular design. The distinct nodal structure of the π -DBS as compared to the σ -DBS also make them candidates as molecular qubits for quantum information science applications. The unique nonadiabatic dynamics mediated by molecular rotation from the σ -DBS to π -DBS further opens up new directions for understanding the electron capture mechanisms by neutral molecules to form molecular anions.

This work was supported by the DOE, Office of Basic Energy Sciences, Chemical Sciences, Geosciences, and Biosciences Division under Grant No. DESC0018679 (to L. S. W.). B. M. R. thanks the Alfred P. Sloan Foundation for their support. We thank Profs. Manfred Kappes, Brad Marston, Dan Neumark, and Peter Weber for valuable discussions. Y. L. was supported by the Brown Presidential Fellowship and the Open Graduate Education Fellowship. The calculation was performed using computational resources and services provided by CCV of Brown University.

*These authors contributed equally to this work.

†To whom all correspondence should be addressed.

Lai-Sheng_Wang@brown.edu

- [1] J. Simons, *J. Phys. Chem. A* **112**, 6401 (2008).
- [2] C. Desfrancois, H. Abdoul-Carime, and J.-P. Schermann, *Int. J. Mod. Phys. B* **10**, 1339 (1996).
- [3] R. N. Compton and N. I. Hammer, in *Advances in Gas Phase Ion Chemistry*, 1st ed. (Elsevier Science, New York, 2001).
- [4] K. D. Jordan and F. Wang, *Annu. Rev. Phys. Chem.* **54**, 367 (2003).
- [5] C. Desfrancois, H. Abdoul-Carime, N. Khelifa, and J. P. Schermann, *Phys. Rev. Lett.* **73**, 2436 (1994).
- [6] N. I. Hammer, K. Diri, K. D. Jordan, C. Desfrancois, and R. N. Compton, *J. Chem. Phys.* **119**, 3650 (2003).
- [7] N. I. Hammer, R. J. Hinde, R. N. Compton, K. Diri, K. D. Jordan, D. Radisic, S. T. Stokes, and K. H. Bowen, *J. Chem. Phys.* **120**, 685 (2004).
- [8] C. H. Qian, G. Z. Zhu, and L. S. Wang, *J. Phys. Chem. Lett.* **10**, 6472 (2019).
- [9] J. Marks, D. M. Wetzel, P. B. Comita, and J. I. Brauman, *J. Chem. Phys.* **71**, 2088 (1979).
- [10] R. L. Jackson, P. C. Hiberty, and J. I. Brauman, *J. Chem. Phys.* **74**, 3705 (1981).
- [11] K. R. Lykke, R. D. Mead, and W. C. Lineberger, *Phys. Rev. Lett.* **52**, 2221 (1984).
- [12] K. Yokoyama, G. W. Leach, J. B. Kim, W. C. Lineberger, A. I. Boldyrev, and M. Gutowski, *J. Chem. Phys.* **105**, 10706 (1996).
- [13] C. Desfrancois, Y. Bouteiller, J. P. Schermann, D. Radisic, S. T. Stokes, K. H. Bowen, N. I. Hammer, and R. N. Compton, *Phys. Rev. Lett.* **92**, 083003 (2004).
- [14] T. Sommerfeld, K. M. Dreux, and R. Joshi, *J. Phys. Chem. A* **118**, 7320 (2014).
- [15] G. Z. Zhu, Y. Liu, and L. S. Wang, *Phys. Rev. Lett.* **119**, 023002 (2017).
- [16] M. Gutowski, P. Skurski, X. Li, and L. S. Wang, *Phys. Rev. Lett.* **85**, 3145 (2000).
- [17] T. Sommerfeld, B. Bhattarai, V. P. Vysotskiy, and L. S. Cederbaum, *J. Chem. Phys.* **133**, 114301 (2010).
- [18] V. G. Bezchastnov, V. P. Vysotskiy, and L. S. Cederbaum, *Phys. Rev. Lett.* **107**, 133401 (2011).
- [19] V. K. Voora, L. S. Cederbaum, and K. D. Jordan, *J. Phys. Chem. Lett.* **4**, 849 (2013).
- [20] V. K. Voora and K. D. Jordan, *J. Phys. Chem. Lett.* **6**, 3994 (2015).
- [21] J. N. Bull and J. R. R. Verlet, *Sci. Adv.* **3**, e1603106 (2017).
- [22] J. P. Rogers, C. S. Anstöter, and J. R. R. Verlet, *Nat. Chem.* **10**, 341 (2018).
- [23] H. Abdoul-Carime and C. Desfrancois, *Eur. Phys. J. D* **2**, 149 (1998).
- [24] K. J. Taylor, C. Jin, J. Conceicao, L. S. Wang, O. Cheshnovsky, B. R. Johnson, P. Norlander, and R. E. Smalley, *J. Chem. Phys.* **93**, 7515 (1990).
- [25] C. D. Finch, R. A. Popple, P. Nordlander, and F. B. Dunning, *Chem. Phys. Lett.* **244**, 345 (1995).
- [26] R. F. Wallis, R. Herman, and H. W. Milnes, *J. Mol. Spectrosc.* **4**, 51 (1960).
- [27] O. H. Crawford, *Proc. Phys. Soc. London* **91**, 279 (1967).
- [28] A. Kairalapova, K. D. Jordan, M. F. Falcetta, D. K. Steiner, B. L. Sutter, and J. S. Gowen, *J. Phys. Chem. B* **123**, 9198 (2019).
- [29] V. K. Voora and K. D. Jordan, *Nano Lett.* **14**, 4602 (2014).
- [30] H. T. Liu, C. G. Ning, D. L. Huang, P. D. Dau, and L. S. Wang, *Angew. Chem., Int. Ed. Engl.* **52**, 8976 (2013).
- [31] D. L. Huang, H. T. Liu, C. G. Ning, and L. S. Wang, *J. Chem. Phys.* **142**, 124309 (2015).
- [32] D. L. Huang, H. T. Liu, C. G. Ning, G. Z. Zhu, and L. S. Wang, *Chem. Sci.* **6**, 3129 (2015).
- [33] D. L. Huang, H. T. Liu, C. G. Ning, and L. S. Wang, *J. Phys. Chem. Lett.* **6**, 2153 (2015).
- [34] G. Z. Zhu, C. H. Qian, and L. S. Wang, *J. Chem. Phys.* **149**, 164301 (2018).
- [35] G. Liu, S. M. Ciborowski, C. R. Pitts, J. D. Graham, A. M. Buytendyk, T. Lectka, and K. H. Bowen, *Phys. Chem. Chem. Phys.* **21**, 18310 (2019).
- [36] G. Liu, S. M. Ciborowski, J. D. Graham, A. M. Buytendyk, and K. H. Bowen, *J. Chem. Phys.* **151**, 101101 (2019).

- [37] M. Feng, J. Zhao, and H. Petek, *Science* **320**, 359 (2008).
- [38] R. N. Compton and H. S. Carman, Jr., C. Defrançois, H. Abdoul-Carmine, J. P. Schermann, J. H. Hendricks, S. A. Lyapustina, and K. H. Bowen, *J. Chem. Phys.* **105**, 3472 (1996).
- [39] T. Sommerfeld, *Phys. Chem. Chem. Phys.* **4**, 2511 (2002).
- [40] A. Kunin and D. M. Neumark, *Phys. Chem. Chem. Phys.* **21**, 7239 (2019).
- [41] R. C. Fortenberry, *J. Phys. Chem. A* **119**, 9941 (2015).
- [42] M. Saffman, T. G. Walker, and K. Mølmer, *Rev. Mod. Phys.* **82**, 2313 (2010).
- [43] L. S. Wang, *J. Chem. Phys.* **143**, 040901 (2015).
- [44] X. B. Wang and L. S. Wang, *Rev. Sci. Instrum.* **79**, 073108 (2008).
- [45] I. León, Z. Yang, H. T. Liu, and L. S. Wang, *Rev. Sci. Instrum.* **85**, 083106 (2014).
- [46] See the Supplemental Material at <http://link.aps.org/supplemental/10.1103/PhysRevLett.125.073003> for more experimental details, data analyses, nonresonant photoelectron spectra, additional resonant photoelectron spectra, theoretical calculations, and additional discussions.
- [47] H. T. Liu, C. G. Ning, D. L. Huang, and L. S. Wang, *Angew. Chem., Int. Ed. Engl.* **53**, 2464 (2014).
- [48] G. Z. Zhu, C. H. Qian, and L. S. Wang, *Angew. Chem., Int. Ed. Engl.* **58**, 7856 (2019).
- [49] G. Z. Zhu and L. S. Wang, *Chem. Sci.* **10**, 9409 (2019).
- [50] R. S. Berry, *J. Chem. Phys.* **45**, 1228 (1966).
- [51] J. Simons, *J. Am. Chem. Soc.* **103**, 3971 (1981).
- [52] D. L. Huang, H. T. Liu, C. G. Ning, P. D. Dau, and L. S. Wang, *Chem. Phys.* **482**, 374 (2017).
- [53] K. F. Freed and A. Nitzan, *J. Chem. Phys.* **73**, 4765 (1980).
- [54] G. Z. Zhu, L. F. Cheung, Y. Liu, C. H. Qian, and L. S. Wang, *J. Phys. Chem. Lett.* **10**, 4339 (2019).
- [55] Other photoexcitation processes could conceivably take place by the second photon, such as a core-excited state. In other word, the second photon excites the 9AT neutral core of the DBS to a valence excited state, which can then autodetach by emitting the dipole-bound electron prepared by the first photon. We considered this possibility and concluded it is unlikely. See the Supplemental Material for additional theoretical calculations and discussions [46].
- [56] W. R. Garrett, *J. Chem. Phys.* **73**, 5721 (1980).
- [57] W. R. Garrett, *J. Chem. Phys.* **77**, 3666 (1982).
- [58] D. L. Huang, G. Z. Zhu, Y. Liu, and L. S. Wang, *J. Mol. Spectrosc.* **332**, 86 (2017).
- [59] D. C. Harris and M. D. Bertolucci, *Symmetry and Spectroscopy: An Introduction to Vibrational and Electronic Spectroscopy* (Dover Publications Inc., New York, 1989).